RSC Advances




ROYAL SOCIETY OF CHEMISTRY

www.rsc.org/advances

Cite this: DOI: 10.1039/c0xx00000x

www.rsc.org/xxxxxx

ARTICLE TYPE

# Photovoltaic properties of 3,3'-(ethane-1,2-diylidene)-bis(indolin-2-one) based conjugated polymers

**Jian Wu[a], Yingying Fu[b], Hao Huang[a], Shengxia Li[a] and Zhiyuan Xie[b,**] and Qing Zhang[a,*]**

***Received (in XXX, XXX) Xth XXXXXXXXX 20XX, Accepted Xth XXXXXXXXX 20XX***

**DOI: 10.1039/b000000x**

3,3'-(Ethane-1,2-diylidene)-bis(indolin-2-one) (EBI) is a π-conjugated structure in which two oxindoles are connected by a 1,3-butadiene. An *N*-alkylated EBI monomer has been synthesized in this study. NMR results showed that two central double bonds of the EBI monomer were in a *Z-Z* configuration. Two new polymers with the EBI and benzodithiophenes (BDTs) as building blocks have been synthesized. The new polymers possess relatively low HOMO energy levels, suitable LUMO energy levels and broad absorption through most of the visible region and extended to near-IR. The polymers have been applied as donor materials in bulk hetero-junction polymer solar cell (PSC) devices. The PSC devices based on the blend of EBI-BDT polymers and $PC_{71}BM$ achieved a power conversion efficiency of 4.59% and a $V_{oc}$ of 0.94 V.

## Introduction

Polymer solar cells (PSCs), possessed with many advantages such as low cost, light-weight construction and solution processing may become an important part of renewable energy in the future.[1-3] Conjugated polymers play a key role for the conversion of solar energy into electrical power in PSCs. The incorporation of appropriate electron-deficient (acceptor) and electron-rich (donor) moieties into a conjugated chain can reduce bandgap and fine-tune HOMO/LUMO energy levels of a polymer, and may achieve high performance materials for PSC applications. Bis-oxindole based monomers such as isoindigo[4, 5] and expanded isoindigo[6,7] have become important building blocks for conjugated polymers recently. Many high-performance organic photovoltaic (OPV) devices[8] and organic thin-film transistor (OTFT) devices[9-11] were based on the materials containing bis-oxindole as building blocks. The common features of bis-oxindole based polymers include low-lying frontier orbital energy levels, strongly absorbing through most of the visible region and extended to near-IR, good solubility after *N*-alkylation and ease of synthesis in large scale.[12,13]

3,3'-(Ethane-1,2-diylidene)-bis(indolin-2-one) (EBI) is a π-conjugated structure in which two oxindoles are connected by a 1,3-butadiene.[14,15] The π-conjugation in EBI is more extended than that in isoindigo which has two oxindoles connected by an ethylene. The EBI structure is less rigid compared with isoindigo because the single bond in the middle could provide some rotational freedom. With these structural characteristics, the EBI is an attractive building block for photovoltaic polymers.

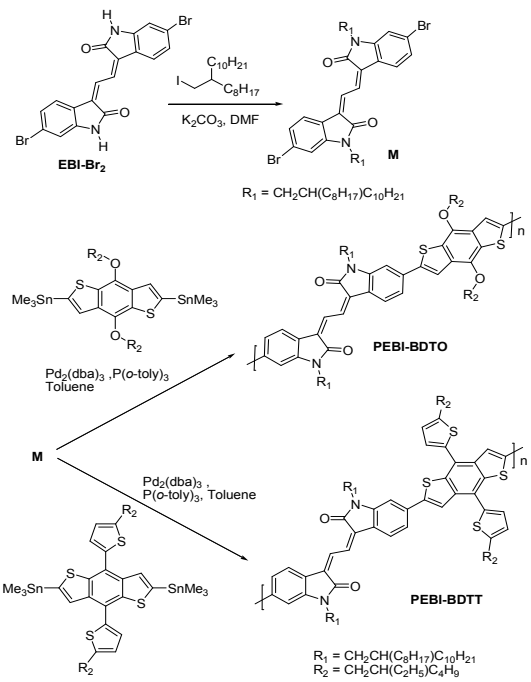


**Scheme 1** Synthetic routes of monomer and polymers

The synthesis of EBI has been known for long time.[15] However, its application as a building block for conjugated polymer has

been reported only recently by Chen and Li.[16] The EBI and bithiophene based polymer showed moderate performance in OTFT devices. However, the photovoltaic property of conjugated polymer based on EBI has never been reported so far. Herein, we present the synthesis of two new polymers based on EBI and benzodithiophenes (BDTs), and the characterization of their thermal, optical and electrochemical properties. The solar cell devices based on the new polymer as the donor and $PC_{71}BM$ as the acceptor achieved a power conversion efficiency (PCE) of 4.59%.

## Experimental section

### Instrument

$^1H$ and $^{13}C$ NMR spectra were measured on a Mercury plus 400 MHz machine. Elemental analyses were performed on an Elementar vario EL III elemental analysis instrument at Shanghai institute of organic chemistry, Chinese academy of sciences. Gel permeation chromatography (GPC) measurements were performed on a Shimadzu LC-20A instrument with tetrahydrofuran as eluent and polystyrenes as standards. Thermogravimetric analyses (TGA) were conducted with a TA instrument Q5000IR at a heating rate of 20 $^oC$ $min^{-1}$ under nitrogen gas flow. Differential scanning calorimetry (DSC) analyses were performed on a Perkin Elmer instrument Pyris 1 in nitrogen atmosphere. All the samples (about 5.0 mg in weight) were first heated to 300 $^oC$ and held for 2 min to remove thermal history, followed by the cooling at rate of 10 $^oC$ $min^{-1}$ to 25 $^oC$ and then heating at rate of 10 $^oC$ $min^{-1}$ to 250 $^oC$. UV-vis spectra were recorded on a Perkin Elmer Lambda 20 UV-vis spectrophotometer. Electrochemical measurements were conducted on a CHI 600 electrochemical analyzer under nitrogen in a deoxygenated anhydrous acetonitrile solution of tetra-*n*-butylammonium hexafluorophosphate (0.1 M). A platinum disc electrode was used as a working electrode, a platinum-wire was used as a counter electrode, and an $Ag/Ag^+$ electrode was used as a reference electrode. The electrode was calibrated with ferrocene/ferrocenium ($Fc/Fc^+$) redox couple as an external standard which was measured under the same conditions before and after the measurement of samples. The thin-film of polymer sample was drop-coated on the surface of platinum disc electrode.

### Computational method

Density functional theory (DFT) calculations for the model molecules using Gaussian 09 at the level of B3LYP/6-31G** were performed, aiming to gain insight into the possible molecular geometries arising from the chemical structures. Only one repeating unit of polymer was subjected to simulation and alkyl chains were replaced by methyl groups in the model compounds for simplifying the calculations.

### Fabrication and characterization of polymer solar cells

Polymer solar cells were fabricated with a conventional device structure of ITO/PEDOT:PSS/polymer:$PC_{71}BM$/LiF/Al. After cleaned and dried at 120℃ in an oven, the ITO substrate was treated with UV-ozone for 25 min. Then, a thin-film of PEDOT:PSS (about 30 nm) was spin-coated, dried at 130℃, and was transferred into a glove box filled with nitrogen. Polymer and $PC_{71}BM$ were dissolved in chlorobenzene (CB). The total concentration of the solutions was kept at 20 mg/ml with varying weight ratios of polymer:$PC_{71}BM$. The solution was filtered through a poly(tetrafluoroethylene) (PTFE) filter (0.45 μm). The active layer was spin-coated on top of the PEDOT/PSS layer from a solution containing a mixture of polymer and $PC_{71}BM$. The samples were transferred into an evaporator, in which lithium fluoride (1.0 nm) and aluminum (100 nm) layers were thermally deposited under a vacuum of $1.0 \times 10^{-6}$ torr through a shadow mask (active area 0.08 $cm^2$). At least nine solar cells were fabricated for each device described in this study. The current-voltage characteristics of the photovoltaic cells were measured with a Keithley 236 source meter. An Oriel solar simulator equipped with an AM 1.5G filter was used to provide an intensity of 100 $mW/cm^2$ for illumination. The external quantum efficiency (EQE) measurement was performed under short circuit conditions using Enlitech QE-R equipment. The thickness of the active layer was obtained by a Dektak surface profiler. The atomic force microscopy (AFM) images were obtained from a SPA-300HV instrument equipped with a SPI3800N Controller (Seiko Instruments Inc., Japan) in tapping mode. Devices for space-charge-limited current (SCLC) measurements were fabricated in a manner similar to the solar cell devices with the structure of ITO/PEDOT:PSS/polymer:$PC_{71}BM$(1:2)/$MoO_3$(10 nm)/Al.

### Materials

All reagents purchased from commercial sources were used without further purification unless otherwise noted. 2,6-Bis(trimethyltin)-4,8-di(2-ethylhexyloxy)-benzo[1,2-b;4,5-b']dithiophene (BDTO) and 2,6-bis(trimethyltin)-4,8-di(2-ethylhexylthiophen-5-yl)-benzo[1,2-b;4,5-b']dithiophene (BDTT) were purchased from Rixun chemical company. Toluene and tetrahydrofuran (THF) were freshly distilled over sodium wire under nitrogen prior to use. 9-(Iodomethyl)nonadecane[17] and 3,3'-(ethane-1,2-diylidene)bis(6-bromoindolin-2-one)[15,16] were prepared according to the methods reported in the literatures.

### Synthesis of the monomers and polymers

**(3Z,3'Z)-3,3'-(Ethane-1,2-diylidene)bis(6-bromo-1-(2-octyldodecyl)indolin-2-one) (M).** 3,3'-(Ethane-1,2-diylidene)-bis(6-bromoindolin-2-one) (4.46 g, 10.0 mmol) and anhydrous potassium carbonate (6.90 g, 50.0 mmol) in *N,N*-dimethylformamide (DMF) (150 mL) were stirred at 120 $^oC$ under $N_2$ atmosphere for 0.5 h. 9-(Iodomethyl)nonadecane (12.24 g，30.0 mmo) was added to the mixture. The reaction mixture was stirred at 80 $^oC$ for 24 h. After cooled to room temperature, the mixture was poured into water and was extracted with dichloromethane. The combined organic phase was washed with water, brine, and was dried with anhydrous magnesium sulfate.

After filtration, the solvent was removed under reduced pressure and the residue was purified by flash chromatography on silica gel with dichloromethane/hexane (1:10) as eluent to give the title compound as a red liquid (5.74 g，57% yield). $^1$H NMR (400 MHz, $CDCl_3$) δ (ppm): 8.95 (s, 2H), 7.47 (d, $J$ = 8.0 Hz, 2H), 7.16(dd, $J$ = 8.0, 1.6 Hz, 2H), 6.90 (d, $J$ =1 .6 Hz, 2H), 3.57(d, $J$ = 7.2 Hz, 4H), 1.87 (m, 2H), 1.20-1.45 (m, 64H), 0.86-0.91 (m, 12H). $^{13}$C NMR (100 MHz, $CDCl_3$) δ (ppm): 167.21, 144.65, 130.35, 129.12, 125.12, 124.59, 122.50, 122.27, 112.17, 44.55, 36.41, 32.13, 31.81, 30.19, 29.86, 29.81, 29.75, 29.57, 29.52, 26.66, 22.90. Anal. Calcd for $(C_{58}H_{90}Br_2N_2O_2)_n$: C 69.17, H 9.01, N 2.78; found: C 69.25, H 8.98, N 2.51%.

**Polymer PEBI-BDTO.** M (0.2022 g, 0.20 mmol), BDTO (0.1544 g，0.20 mmol), tris(dibenzylideneacetone) dipalladium (0.0037 g, 0.0040 mmol), tri(*o*-tolyl)phosphine (0.0048 g, 0.0160 mmol) and degassed toluene (12.0 mL) were added to a Schlenk tube. The solution was subjected to three cycles of evacuation and admission of nitrogen and was stirred at 100 ℃ for 2 h. After cooled to room temperature, the mixture was poured into methanol (60 mL) and was stirred for 1 h. A deep blue precipitate was collected by filtration. It was washed with methanol and hexane in a Soxhlet extractor for 24 h each. It was extracted with hot chloroform in an extractor for 24 h. After removing the solvent, a dark blue solid with a metallic luster was collected (0.212 g, 82 % yield). $^1$H NMR (400 MHz, $CDCl_3$) δ (ppm): 8.6-6.8(br), 4.3-4.0(br), 3.7-3.4(br), 2.1-0.6(br). Anal. Calcd for $(C_{84}H_{126}N_2O_4S_2)_n$: C 78.09, H 9.83, N 2.17; found: C 77.50, H 9.88, N 2.00%.

**Polymer PEBI-BDTT.** M (0.2022 g，0.20 mmol), BDTT (0.1809 g，0.20 mmol), tris(dibenzylideneacetone) dipalladium (0.0037 g, 0.0040 mmol), tri(o-tolyl)phosphine (0.0048 g, 0.0160 mmol) and degassed toluene (10.0 mL) were added to a Schlenk tube. The solution was subjected to three cycles of evacuation and admission of nitrogen and was stirred at 100 ℃ for 2 h. After cooled to room temperature, the mixture was poured into methanol (60 mL) and was stirred for 1 h. A deep blue precipitate was collected by filtration. It was washed with methanol and hexane in a Soxhlet extractor for 24 h each. It was extracted with hot chloroform in an extractor for 24 h. After removing the solvent, a dark blue solid with a metallic luster was collected (0.222 g，78 % yield). $^1$H NMR (400 MHz, $CDCl_3$) δ (ppm): 6.8-8.5(br), 4.3-4.0(br), 3.7-3.4(br), 2.1-0.6(br). Anal. Calcd for $(C_{92}H_{130}N_2O_2S_4)_n$: C 77.58, H 9.20, N 1.97; found: C 77.60, H 9.39, N 1.82

**Table 1.** Molecular weights and thermal properties of polymers

| Polymer | Yield (%) | $M_n$[a] (kDa) | $M_w$[a] (kDa) | PDI[a] | $T_d$[b] (℃) |
|---|---|---|---|---|---|
| **PEBI-BDTO** | 82% | 50.7 | 111.7 | 2.2 | 277 |
| **PEBI-BDTT** | 78% | 61.8 | 133.9 | 2.2 | 333 |

[a]Number-average molecular weight ($M_n$), weight-average molecular weight ($M_w$), and polydispersity index (PDI) of polymers were determined by GPC using polystyrene as standards with THF as eluent. [b] The temperature of 5% weight-loss under a nitrogen atmosphere.

## Results and Discussion

### Synthesis and structural characterization

The synthetic routes for monomer and polymers are shown in Scheme 1. The 3,3'-(ethane-1,2-diylidene)bis(6-bromoindolin-2-one) (EBI-$Br_2$) was synthesized by condensation of 6-bromoindoline-2,3-dione and propionic anhydride in the present of pyridine according to literatures.[15] The product of the condensation reaction can exist in three stereo isomeric forms, *Z-Z, E-Z*, and *E-E*, considering the vinylic hydrogens and the amide carbonyl groups as reference points.[15] The product showed low solubility in common solvents. So, it was reacted with 9-(iodomethyl)nonadecane in DMF to give the *N*-alkylated product (M).[16] The branched side-chains improved the solubility of the material. The structure of the product was characterized with NMR technique. The *E-Z* isomer can be eliminated easily. However, making a distinction between *Z-Z* and *E-E* isomers unequivocally was difficult according to early study.[15] NOESY and HMBC (hetero-nuclear multiple bond correlation) experiments were carried out on the M, but the results were not conclusive for the assignment of stereo structure. However, the M showed an extraordinary vinylic proton signal at 8.95 ppm on $^1$H NMR spectrum. The large downfield shift was due to the strong de-shielding effect of magnetic anisotropy of carbonyl groups. This effect is significant in conformationally rigid α,β-unsaturated carbonyl compounds and amides. Quite large downfield shifts can be observed when proton is γ to the carbonyl. The effect is reliable enough to be used for structure assignments[18, 19] The vinylic protons in the *Z-Z* isomer are γ to the carbonyl and vinylic protons in the *E-E* isomer are β to the carbonyl. The *E-E* isomer can be excluded due to the appearance of huge downfield shift of the vinylic proton signal in $^1$H NMR spectrum. So, the double bonds in M are in *Z-Z* configuration. This assignment of stereo structure is contrary to a recent report in which an *E-E* isomer has been presumed.[16]

Two donor-acceptor type polymers, **PEBI-BDTO** and **PEBI-BDTT** were synthesized via by Stille cross-coupling reactions with 1:1 monomer ratio in presence of tris(dibenzylideneacetone)-dipalladium as catalyst, tri-*o*-tolylphosphine as ligand and toluene as solvent. The crude polymers were purified by precipitating in methanol and washing with methanol and hexane in a Soxhlet extractor. Both polymers are soluble in common organic solvents such as chloroform (CF), chlorobenzene (CB) and tetrahydrofuran (THF). Polymers were characterized by $^1$H NMR (fig. S3 and S4) and elemental analysis. The number-average molecular weights ($M_n$) and poly-dispersity indexes (PDIs) of the polymers were determined by gel permeation chromatography (GPC) using polystyrenes as standards with THF as eluent. The results are listed in Table 1. The $M_n$ of **PEBI-BDTO** and **PEBI-BDTT** was 50.7 and 61.8 kDa. The PDI of **PEBI-BDTO** and **PEBI-BDTT** was 2.2 and 2.2, respectively.

### Thermal properties

Thermal gravimetric analysis (TGA) was employed to evaluate the thermal stability of the new polymers. The TGA curves are shown in Fig. S5 and the results are listed in Table 1. The temperature of 5% weight-loss was chosen as the onset point of decomposition ($T_d$). The $T_d$ of **PEBI-BDTO** and **PEBI-BDTT** was at 277 and 333 ℃, respectively. The **PEBI-BDTO** was less stable than **PEBI-BDTT** in TGA study due to alkoxy substitutions in the polymer. The both polymers exhibited adequate thermal stability for PSC or other optoelectronic device applications. No noticeable phase transitions were observed for either polymer in differential scanning calorimetry (DSC) study within the range of 30-250 ℃ (Fig.S6).

### Optical properties

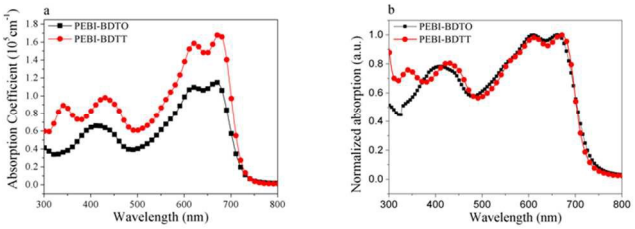


**Fig. 1** UV-vis spectra of polymers (a) in chloroform and (b) as thin-films

The UV-vis absorption spectra of **PEBI-BDTO** and **PEBI-BDTT** in dilute chloroform (CF) solution and as thin films on quartz substrates are shown in Fig. 1. The optical properties of the polymers are listed in Table 2. Both polymers showed absorption bands at high energy region which were corresponded to π–π* transitions, and absorption bands at lower energy region which were due to intramolecular charge transfer (ICT) between EBI (acceptor) and BDT (donor) units.[20-22] The absorption maximum ($\lambda_{max}^{abs}$) of **PEBI-BDTO** and **PEBI-BDTT** in chloroform solution were at 663 nm ($\varepsilon = 1.14\times10^5$ M$^{-1}$cm$^{-1}$) and 668 nm ($\varepsilon = 1.70\times10^5$ M$^{-1}$cm$^{-1}$), respectively. The solution absorption spectra of **PEBI-BDTO** and **PEBI-BDTT** were similar in shape, but the **PEBI-BDTT** showed relatively large extinction coefficient compared with **PEBI-BDTO**. From solution to thin-film, the absorption bands became broader for both polymers. The absorption maximum of the **PEBI-BDTO** and **PEBI-BDTT** thin-films were slightly red-shifted compared with their solution absorption maximum. The absorption onsets of **PEBI-BDTO** and **PEBI-BDTT** thin-films were at 750 and 740 nm. The optical gaps ($E_g$) of the polymers were calculated from the onsets of thin films spectra. The optical bandgaps of **PEBI-BDTO** and **PEBI-BDTT** were 1.65 and 1.67 eV, respectively. It had been reported that the bandgaps of isoindigo-BDT polymers were 1.62 and 1.56 eV for alkoxy substituted[23] and thienyl substituted BDT[24], respectively. The EBI-BDT based polymers showed slightly large bandgaps compared with isoindigo-BDT counter-parts.

### Electrochemical properties

The electrochemical properties of polymers were investigated by cyclic voltammetry (CV). The CV curves of **PEBI-BDTO** and **PEBI-BDTT** films are shown in Fig. 2 and the results are summarized in Table 2. The potentials were referenced to the ferrocene/ferrocenium redox couple ($Fc/Fc^+$). The redox potential of $Fc/Fc^+$ was assumed an absolute energy level of -4.8 eV to vacuum.[25] The redox potential of $Fc/Fc^+$ was measured under the same condition as polymer samples and was located at 0.09 V related to the $Ag/Ag^+$ electrode. The electro-chemical potentials were converted to the corresponding HOMO and LUMO energy levels by the following equations: [26]

$$E_{HOMO} = -(4.8 - E_{1/2,Fc,Fc+} + E_{ox,onset}) = -(4.71 + E_{ox,onset})\ eV$$
$$E_{LUMO} = -(4.8 - E_{1/2,Fc,Fc+} + E_{red,onset}) = -(4.71 + E_{red,onset})\ eV$$

The onset oxidation potentials of **PEBI-BDTO** and **PEBI-BDTT** were at 0.75 and 0.80 V, respectively. The corresponding HOMO energy levels of **PEBI-BDTO** and **PEBI-BDTT** were at 5.46 and 5.51 eV, respectively. The HOMO level of **PEBI-BDTT** was lower than that of **PEBI-BDTO** due weak electron donating strength of BDTT compared with that of BDTO. The deep HOMO levels of the polymers are favorable for achieving high open-circuit voltage ($V_{oc}$) in PCS devices.[27] The onset reduction potentials of **PEBI-BDTO** and **PEBI-BDTT** were at -1.13 and -1.05 V, and the LUMO energy levels were at -3.58 and -3.66 eV, respectively. The LUMO energy levels of the polymers are suitable for PCBMs based bulk hetero-junction PSC applications.

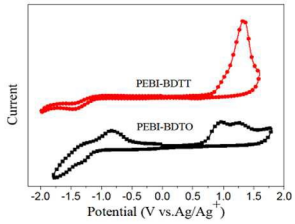


**Fig. 2** Cyclic voltammograms of polymers thin films.

### Theoretical calculations

The theoretical calculation using DFT (B3LYP/6-31G** level) method was employed to study the electronic structures of these polymers. To simplify the calculations, long alkyl side chains were replaced by methyl groups. The results are in Fig. S7. It was found that the HOMO orbits were distributed along the whole structures for both models, while the LUMO orbits were localized at the EBI units for both models. The dihedrals angle between EBI and BDT were 23.65° for **PEBI-BDTO** and 25.04° for **PEBI-BDTT.**

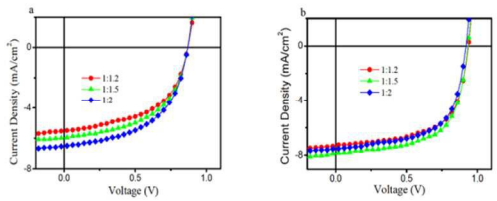


**Fig. 3** *I-V* curves of solar cell devices with different weight ratios of polymer/$PC_{71}BM$, ( a) **PEBI-BDTO**:$PC_{71}BM$ and (b) **PEBI-BDTT**:$PC_{71}BM$.

**Table 2.** Optical and electrochemical properties of polymers

| Polymer | Solution λ (nm) | Film λ (nm) | | p & n-Doping (V *vs*. $Ag/Ag^+$) | | | | Bandgap (eV) | |
|---|---|---|---|---|---|---|---|---|---|
| | $\lambda_{max}^{abs}$ (nm) | $\lambda_{max}^{abs}$ (nm) | $\lambda_{onset}^{abs}$ (nm) | $E_{onset}^{ox}$ (V) | HOMO (eV) | $E_{onset}^{red}$ (V) | LUMO (eV) | $E_g^{opt}$ (eV)[c] | $E_g^{CV}$ (eV)[d] |
| **PEBI-BDTO** | 663 | 667 | 750 | 0.75 | -5.46 | -1.13 | -3.58 | 1.65 | 1.88 |
| **PEBI-BDTT** | 668 | 676 | 740 | 0.80 | -5.51 | -1.05 | -3.66 | 1.67 | 1.85 |

**Photovoltaic properties**

Polymer solar cell devices with polymer **PEBI-BDTO** and **PEBI-BDTT** as electron donors and $PC_{71}BM$ as electron acceptor were fabricated. The device structures were ITO/PEDOT:PSS/polymer:$PC_{71}BM$/LiF/Al and the photovoltaic performances were measured under the illumination with AM 1.5G simulated solar light at 100 mW/cm$^2$. The solar cell devices with active layer thickness of 65, 90, 120, and 150 nm were fabricated and tested. Devices with thickness of 120 nm showed the best photovoltaic performances. In many high efficient polymer solar cells, a small amount of 1,8-diiodooctane (DIO) is used as processing additive for achieving a suitable interpenetrating network.[24, 27-29] Therefore, we studied the effect of DIO on the devices performances (table S1). As a consequence, the addition of diiodooctane (DIO) improved the device performances in both **PEBI-BDTO:$PC_{71}BM$** and **PEBI-BDTT:$PC_{71}BM$** based solar cells and the best performances were achieved with addition of 3% DIO (by volume). The devices with different weight ratios of polymers to $PC_{71}BM$ in active layer were fabricated from chlorobenzene solution with DIO as addictive. The current density/voltage (*I-V*) characteristics ofthese solar cell devices are displayed in Fig. 3 (a) and (b), and the photovoltaic performances are listed in Table 3. At 1:2 weight ratio of polymer/$PC_{71}BM$, the **PEBI-BDTO** based devices showed the best performance, with a $V_{oc}$ of 0.86 V, a $J_{sc}$ of 6.53 mA/cm$^2$, a FF of 53.3% and a PCE of 3.00%. At 1: 1.5 weight ratio of polymer/$PC_{71}BM$, the **PEBI-BDTT** showed the best performance with a $V_{oc}$ of 0.94 V, a $J_{sc}$ of 7.88 mA/cm$^2$, a FF of 62.1% and a PCE of 4.59%. The **PEBI-BDTT** based devices showed relatively high $V_{oc}$ compared with **PEBI-BDTO** based devices due to deep HOMO energy level of **PEBI-BDTT**. The photovoltaic performances of **PEBI-BDTT** were better than those of **PEBI-BDTO**. This could result from combined factors,

**Table 3.** Photovoltaic performance of the solar cell devices.

| Active layer D/A | D:A (w/w) | Jsc (mA/cm$^2$) | Voc (V) | FF (%) | PCE (%) |
|---|---|---|---|---|---|
| | 1:1.2 | 5.51 | 0.86 | 53.5 | 2.54±0.11 |
| **PEBI-BDTO**/$PC_{71}BM$ | 1:1.5 | 5.98 | 0.86 | 53.3 | 2.74±0.06 |
| | 1:2 | 6.53 | 0.86 | 53.4 | 3.00±0.12 |
| | 1:1.2 | 7.32 | 0.94 | 61.5 | 4.23±0.20 |
| **PEBI-BDTT**/$PC_{71}BM$ | 1:1.5 | 7.88 | 0.94 | 62.1 | 4.59±0.15 |
| | 1:2 | 7.53 | 0.92 | 61.1 | 4.23±0.18 |

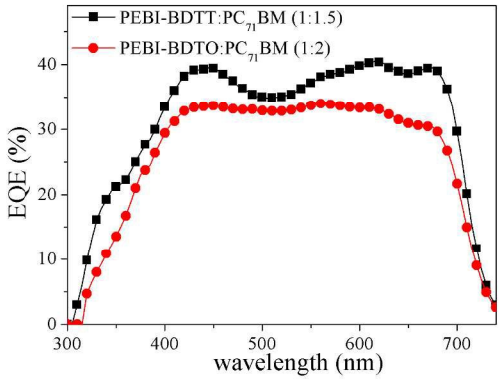


**Fig. 4** EQE curves of solar cell devices.

such as better photon absorption, lower HOMO energy level and higher charge mobility. Similar observations have reported on other polymers based on alkoxy and thienyl substituted BDT.[28, 29] The external quantum efficiencies (EQE) of the devices were measured. The results are shown in Fig. 4. The devices based on **PEBI-BDTO** and **PEBI-BDTT** displayed broad response ranges covering from 300 to 750 nm. The **PEBI-BDTT** based devices showed the EQE peak value of 40%, and **PEBI-BDTO** based devices showed the EQE peak value of 34%. The calculated $J_{sc}$ from EQE values of devices were 6.30 and 7.56 mA/cm$^2$ for **PEBI-BDTO** and **PEBI-BDTT** based devices, respectively, which perfectly matched the values measured from *J-V* characteristics.

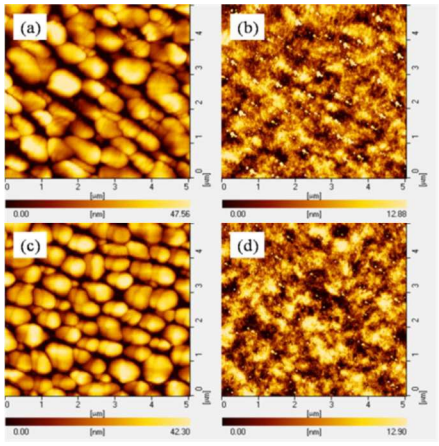


**Fig. 5** AFM topography images of **PEBI-BDTO**:$PC_{71}BM$ (1:2) without (a) and with DIO (b), **PEBI-BDTT**:$PC_{71}BM$ (1:1.5) without (c) and with DIO (d).

The effect of additive, DIO on the film morphology was studied by atomic force microscopy (AFM).[30-32] The AFM topography images were taken for the films of **PEBI-BDTO**/$PC_{71}BM$ and **PEBI-BDTT**/$PC_{71}BM$ with or without DIO (Fig. 5). The blend films based on **PEBI-BDTO**/$PC_{71}BM$ and **PEBI-BDTT**/$PC_{71}BM$ showed very large aggregations when spin-coated without DIO (Fig. 5a and 5c). The large aggregations could be attributed to the poor miscibility between the donor polymers and $PC_{71}BM$. The domain sizes were more than several hundred nanometers, which were much larger than the scale of exciton diffusion, inducing low efficiency of exciton dissociation. After addition of small amount of DIO (3% by volume), the aggregations in the two blend films were both suppressed and the domain sizes were significantly reduced (Fig. 5b and 5d). The photo-generated charges increased and $J_{sc,}$ PCE of PSCs improved.

### Charge Transport in Polymer/$PC_{71}BM$ Blends

Hole-only devices were fabricated with the configuration of ITO/PEDOT:PSS/polymer:$PC_{71}BM$/$MoO_3$/Al. The hole mobilities were measured by space charge limited current (SCLC) method and were calculated by following equation:

$$J = \frac{9}{8}\varepsilon\varepsilon_0\mu\exp(\gamma\sqrt{\frac{V}{L}})\frac{V^2}{L^3}$$

where $J$ is the current density, $V$ is the applied voltage, $L$ is the thickness of the active layer, $\mu$ is the mobility, $\varepsilon$ is the dielectric constant, $\varepsilon_0$ is the permittivity of free space, and $\gamma$ is the field activation factor. The relationship between current and voltage in the hole-only devices is shown in Fig. S9 and the calculated hole mobilities were $7.55\times10^{-5}$ and $1.02\times10^{-4}$ $cm^2V^{-1}s^{-1}$ for **PEBI-BDTO** and **PEBI-BDTT**, respectively.

### Conclusions

In summary, *N*-alkylated EBI monomer has been synthesized. The monomer has two double bonds in a *Z-Z* configuration based on NMR study. This assignment of stereo structure is different from a recent report in which an *E-E* isomer has been presumed. Two new polymers, **PEBI-BDTO** and **PEBI-BDTT** have been synthesized. The EBI based conjugated polymers possess relatively low HOMO energy levels, suitable LUMO energy levels and broad absorption through most of the visible region and extended to near-IR. These material properties are desirable for PSC applications. Polymer solar cell devices with the new polymers as donors and $PC_{71}BM$ as acceptor were fabricated and tested. The morphologies of the active layers can be effectively optimized by addition of DIO. The **PEBI-BDTT** based device achieved a PCE of 4.59% and a Voc of 0.94 V. This work has demonstrated that the EBI is a promising building block for photovoltaic polymers.

### Acknowledgements

This work was supported by National Natural Science Foundation of China (NSFC Grant Nos. 21174084, 21274087, 51325303) and by Doctoral Fund of Ministry of Education of China (Grant No. 20120073110032).

### Notes and references

[a]*Shanghai Key Lab of Polymer and Electrical Insulation, School of Chemistry and Chemical Engineering, Shanghai Jiaotong University, Shanghai 200240, P. R. China*

[b]*State Key Laboratory of Polymer Physics and Chemistry, Changchun Institute of Applied Chemistry, Chinese Academy of Sciences, Changchun, 130022, P.R. China.*

*Corresponding author. Tel.: +86 21 3420 2726.

**Corresponding author. Tel.: +86 431 85262819.

*E-mail addresses*: qz14@sjtu.edu.cn (Q. Zhang), xiezy_n@ciac.ac.cn (Z. Xie).

1 J. Pee, A.J. Heeger and G. C. Bazan, *Acc. Chem. Res.* 2009, **42**, 1700.

2 M. Helgesen, R. Søndergaard and F. C. Krebs, *J. Mater. Chem.* 2010, **20**, 36.

3 C. J. Brabec, S. Gowrisanker, J. J. M. Halls, D. Laird, S. Jia and S. Williams, *Adv. Mater.* 2010, **22**, 3839.

4 Y. F. Deng, J. Liu, J. T. Wang, L. H. Liu, W. L. Li, H. K. Tian, X. J. Zhang, Z. Y. Xie, Y. H. Geng and F. S. Wang, *Adv. Mater.* 2014,**26**, 471.

5 E. G. Wang, Z. F. Ma, Z. Zhang, P. Henrriksson, O. Inganäs, F. L. Zhang and M. R. Andersson, *Chem. Commun.* 2011, **47**, 4908.

6 Z. Q. Yan, B. Sun and Y. N. Li, *Chem. Commun.* 2013, **49**, 3790.

7 W. Hong, C. Guo, B. Sun and Y. N. Li , *J. Mater. Chem. C*, 2015, **3**, 4464.

8 S. G. Li, Z. C.Yuan, J. Y. Yuan, P. Deng, Q. Zhang and B. Q. Sun , *J. Mater. Chem. A*, 2014, **2**, 5427.

9 T. Lei, J. H. Dou, X. Y. Cao, J. Y. Wang and J. Pei, *Adv. Mater.* 2013, **25**, 6589.

10 Y. Cao, J. S. Yuan, X. Zhou, X. Y. Wang, F. D. Zhuang and J. Y. Wang, J. Pei , *Chem. Commun.* 2015, **51**, 10514.

11 S. Holliday, J. E. Donaghey and I. McCulloch, *Chem. Mater.* 2014, **26**, 647.

12 E. Wang , W. Mammo and M. R. Andersson, *Adv. Mater.* 2014, **26**, 1801.

13 P. Deng and Q. Zhang, *Polym. Chem.* 2014, **5**, 3298.

14 T. Lei, J. Yu and J. Pei, *Acc. Chem. Res.* 2014, **47**, 1117.

15 A. W. Johnson and A. S. Katner, *J. Chem. Soc.* 1965, **256**, 1455.

16 S. Y. Chen, B. Sun, C. Guo, W. Hong, Y. Z. Meng and Y. N. Li , *Chem. Commun.* 2014, **50**, 6509.

17 J. A. Letizia, M. R. Salata, C. M. Tribout, A. Facchetti, M. A. Ratner and T. J. Marks, *J. Am. Chem. Soc.* 2008, **130**, 9679.

18 G. C. Paul and J. J. Gajewski, *J. Org. Chem.* 1992, **57**, 1970.

19 L. Emst and R. Stolle, *Magn. Res. Chem.* 1989, **27**, 796.

20 W. Y. Zhou, Z. G. Zhang, L. C. Ma, Y.F. Li and X. W. Zhan, *Sol. Energy Mater. Sol. Cells*, 2013, **112**, 13.

21 M. X. Wan, H. B. Zhu, J. Liu and L. J. Huo, *RSC Adv.* 2015, **5**, 269.

22 B. C. Schroeder, M. Kirkus, C. B. Nielsen, R. S. Ashraf and I. McCulloch, *Macromolecules*, 2015, **48**, 5557.

23 G. B. Zhang, Y. Y. Fu, Z. Y. Xie and Q. Zhang, *Macromolecules*,

2011, **44,** 1414.
24 K. L. Cao, Z. W. Wu, S. G. Li, B. Q. Sun, G. B. Zhang and Q. Zhang, *J. Polym. Sci. Part A: Polym. Chem*. 2013, **51**, 94.
25 J. Pommerehne, H. Vestweber, W. Guss, R. F. Mahrt, H. Bässler and M. Porsch, J. Daub, *Adv. Mater*. 1995, 7, 551.
26 Y. F. Li, Y. Cao, J. Gao, D. Wang, G. Yu and A. J. Heeger, *Synth. Met*. 1999, **99**, 243.
27 R. Stalder, J. Mei, K. R. Graham, L. A. Estrada and J. R. Reynolds, *Chem. Mater*. 2014, **26**, 664.
28 L. J. Huo, S. Q. Zhang, X. Guo, F. Xu, Y. L. Li and J. H. Hou, *Angew. Chem. Int. Ed*. 2011, **50**, 9697.
29 J. H. Kim, J. B. Park, F. Xu, D. W. Kim, J. H. Kwak, A. C. Grimsdale and D. H. Hwang, *Enery Environ. Sci*. 2014, **7**, 4118.
30 D. Kitazawa, N. Watanabe, S. Yamamoto and J. Tsukamoto, *Sol. Energy Mater. Sol. Cells*,2012, **98**, 203.
31 B. L. Hu, M. M. Li, W. Q. Chen, X. J. Wan, Y. S. Chen and Q. H. Zhang, *RSC Adv*. 2015, 5, 50137.
32 L. Huo, L. Yi, Y. Wu, Z. Li, X. Guo, M. Zhang and S. Zhang, J. Hou, *Macromolecules*, 2012, **45**, 6923.

**Photovoltaic properties of 3,3'-(ethane-1,2-diylidene)-bis(indolin-2-one) (EBI) based conjugated polymers.**